

**Residual Dipolar Coupling Measurements of Transmembrane Proteins Using
Aligned Low-q Bicelles and High-Resolution Magic Angle Spinning NMR
Spectroscopy**

Christian G. Canlas, Dejian Ma, Pei Tang, Yan Xu*

Departments of Anesthesiology, Pharmacology, and Structural Biology

University of Pittsburgh School of Medicine, Pittsburgh, PA 15260

A. Properties of Low-q Bicelles ($q \sim 0.5$).

The theory of nematic phase transition, which is beyond the scope of this paper, can be found in the seminal paper by Lars Onsager¹. Onsager particularly considered the possibility of rod-shaped particles, such as lipid molecules, to form a nematic phase at relatively low concentrations where orientation of the particles is anisotropic while the spatial distribution of the particles is homogeneous. It was shown that the transition from an isotropic to an anisotropic phase occurs when the following condition is met:

$$\sigma(f) + bc\rho(f) = \text{minimum} \quad (\text{S1})$$

where b and c are the covolume and the concentration of the colloidal particles, $f = f(\mathbf{a})$ is the angular distribution function within the solid angle $d\Omega(\mathbf{a})$ defined by the unit vector \mathbf{a} , and the functional σ and ρ are given by

$$\sigma(f) = \int f(\mathbf{a}) \log[4\pi f(\mathbf{a})] d\Omega(\mathbf{a}) \quad (\text{S2})$$

and

$$-2b\rho(f) = \iint \beta_1[\cos^{-1}(\mathbf{a}\mathbf{g}\mathbf{a}')] f(\mathbf{a}) f(\mathbf{a}') d\Omega d\Omega' \quad (\text{S3})$$

The distribution function is subject to the restriction

$$\int f(\mathbf{a}) d\Omega(\mathbf{a}) = 1 \quad (\text{S4})$$

For isotropic orientation distribution, $f = f_0 = 1/4\pi$, and expression of the left-hand side of Eq. S1 becomes $\sigma(f_0) + bc\rho(f_0) = bc$. If isotropic to anisotropic transition occurs, the condition in Eq. S1 becomes

$$\sigma(f) + bc\rho(f) < bc \quad (\text{S5})$$

Many angular distribution functions can potentially satisfy S5. The exact analytical solutions, if exist, prove to be quite complicated. Onsager provided numerical

Supporting Information

solutions to special situations with a number of approximations. The salient point of Onsager's approach is that each colloidal particle will claim a maximum volume (the excluded volume) significantly larger than what it actually occupies.

Using this concept, an intuitive approach to estimating the isotropic and nematic phase separation was suggested by Struppe and Vold². Assuming that bicelles have already formed. The condition of inequality in Eq. S5 can be considered by comparing two ratios, the first being the ratio of the excluded volume to the actual volume of a bicelle, and the second being the ratio of the averaged occupiable volume allocated for each lipid to the actual volume occupied by each lipid in a monodispersed isotropic solution. If the latter is larger, an isotropic phase is preferred. Otherwise, a nematic bicelle phase will form. Mathematically, this can be written as:

$$\frac{V_{excl}}{V_{bic}} \geq \frac{V_{total} / N}{b_{lipid}} \approx \frac{V_{total} / N}{\frac{l}{d} V_{lipid}} \approx \frac{1}{\frac{l}{d} c_L} \quad (S6)$$

where b_{lipid} and V_{lipid} are the covolume and the average volume of a lipid, l and d are the length and diameter of the lipid molecule, and c_L is the total lipid concentration (in w/w). The approximation in the second step uses the Onsager's estimation of $b/V \sim l/d$ ($l \gg d$) for a long cylindrical particle, and the approximation in the last step assumes that the lipid and solvent densities are similar.

Let us consider an ideal bicelle where the planar region and the rim are separately occupied by the long-chain (DMPC) and short chain (DHPC) lipids. The q ratio can be written as the ratio of the total areas of the planar to rim region normalized by the area per lipid for DMPC (0.6 nm^2) and DHPC (1.0 nm^2), respectively. Rearranging the ratio to express the radius of the bicelle planar region (R) as a function of q , Vold^{3,4} showed that

$$R_{bicelle} = \frac{rq}{2k} \left(\pi + \sqrt{\pi^2 + \frac{8k}{q}} \right) \quad (S7)$$

where r is the radius of bicelle rim (the length of DHPC, $\sim 2 \text{ nm}$), and k is the area-per-lipid ratio of DHPC to DMPC.

According to Onsager¹, the excluded volume of a disk is:

$$V_{excluded} = \pi(R+r) \left[2r^2 + (\pi+3)r(R+r) + \frac{\pi}{2}(R+r)^2 \right] \quad (S8)$$

The calculation of a bicelle volume is elementary and gives

$$V_{bicelle} = \pi r \left(2R^2 + \pi Rr + \frac{4}{3}r^2 \right) \quad (S9)$$

Supporting Information

For bicelles having $q = 0.5$ and $l/d \sim 2.3$, the values obtained using the equations above are:

$$\begin{array}{ll}
 R_{\text{bicelle}} = 2.76 \times 10^{-9} \text{ m} & R_{\text{bicelle+TM23}} = 4.16 \times 10^{-9} \text{ m} \\
 V_{\text{bicelle}} = 2.38 \times 10^{-25} \text{ m}^3 & V_{\text{bicelle+TM23}} = 4.15 \times 10^{-25} \text{ m}^3 \\
 V_{\text{excluded(bicelle)}} = 1.52 \times 10^{-24} \text{ m}^3 & V_{\text{excluded(bicelle+TM23)}} = 2.77 \times 10^{-24} \text{ m}^3 \\
 c_{L(\text{min})} = 6.8\% & c_{L(\text{min})} = 6.5\%
 \end{array}$$

Our sample has a total lipid concentration of 13-15%, and thus in the nematic bicelle phase.

Struppe and Vold considered a more stringent phase transition condition than Eq. S6, with the second ratio for comparison being the total volume of the solution to the packed volume of lipids. They found experimentally that the concentration of phospholipids leading to nematic bicelle phase is actually much smaller than the minimum concentration given by their stringent transition condition².

B. Chemical Shift Assignment

Table S1. Chemical shift assignment of TM23 in bicelle with $q = 0.5$

Residue	C	C α	C β	HN	H α	N
P2	176.2	63.13	32.14	-	-	-
A3	178.0	53.14	19.27	8.480	4.272	125.1
R4	176.5	56.65	30.75	8.367	4.307	118.5
V5	176.4	63.20	32.65	7.978	4.085	120.0
G6	174.3	45.93	-	8.356	3.957	110.7
L7	178.1	56.01	42.63	8.158	4.345	121.4
G8	175.9	46.06	-	8.365	3.978	109.0
I9	174.0	62.51	38.49	8.092	4.382	120.0
T10	175.8	64.48	69.02	8.413	4.263	117.6
T11	175.3	64.34	69.32	8.026	4.228	117.5
V12	175.6	64.83	32.15	7.911	4.005	120.5
L13	178.1	56.39	42.15	8.167	4.397	121.5
T14	175.0	63.92	69.56	8.026	4.294	114.5
L15	177.7	56.38	42.68	8.057	4.384	122.7
T16	175.0	62.36	69.94	8.026	4.395	113.2
T17	174.8	62.41	69.99	7.940	4.348	114.4
Q18	176.2	56.35	29.50	8.241	4.431	121.9
S19	174.8	58.59	64.03	8.299	4.496	116.5

Supporting Information

S20	175.2	58.90	64.01	8.330	4.483	117.5
G21	176.0	45.54	-	8.393	4.477	111.0
S22	174.7	58.62	64.03	8.118	4.462	114.7
R23	176.0	56.35	30.74	8.320	4.371	122.5
A24	177.3	52.72	19.41	8.169	4.352	124.2
S25	174.0	58.14	64.20	8.107	4.476	114.5
L26	-	53.44	41.95	8.115	4.626	124.2
K28	177.0	-	-	-	-	-
V29	-	-	-	7.964	4.150	119.1
S30	-	-	-	8.397	3.983	111.4
Y31	177.6	-	-	-	-	-
V32	-	-	-	7.815	-	119.5
W38	177.1	-	-	-	4.210	-
L39	-	-	-	7.967	-	121.0
V41	-	-	-	-	-	-
C42	176.4	-	-	-	4.459	-
L43	-	-	-	8.314	-	120.9
A49	-	-	-	-	-	-
L50	-	-	-	-	4.239	-
L51	176.8	55.01	42.32	8.446	4.255	119.1
E52	-	56.27	30.20	8.105	-	121.2
Y53	-	57.18	39.59	-	-	-
A54	-	52.87	19.33	8.533	4.314	126.4
A55	177.2	52.89	19.35	8.358	4.134	107.0
V56	-	55.49	29.39	8.389	-	120.7
N57	-	53.29	-	8.529	-	120.4
R61	-	-	-	-	-	-
K62	-	-	-	7.895	-	120.5
K64	-	56.88	33.02	-	-	-
K65	176.6	56.82	33.09	8.089	-	121.3
H66	175.0	55.85	29.30	8.375	-	119.3
R67	176.1	56.54	31.02	7.916	4.307	121.5
L68	177.0	55.54	42.49	8.288	4.327	123.6
L69	-	55.19	42.41	8.146	4.325	122.7
E70	175.9	56.06	30.19	-	-	-
H71	174.2	55.23	29.22	8.489	4.664	119.3
H72	174.0	55.44	29.31	8.675	4.683	119.8
H73	174.2	55.65	29.47	8.536	4.662	120.4

Supporting Information

H74	173.5	55.30	29.24	8.576	4.675	119.4
H75	174.2	55.66	29.59	8.351	4.658	125.4
H76	-	55.42	29.31	8.692	4.688	120.4

C. Summary of RDC Values

Table S2. List of the measured ^{15}N - ^1H , $^{13}\text{C}_\alpha$ - $^1\text{H}_\alpha$, and $^{13}\text{C}_\alpha$ - $^{13}\text{C}'$ RDC values for TM23 aligned in bicelles with $q = 0.5$.

Residue	RDC (^{15}N - ^1H)	RDC ($^{13}\text{C}_\alpha$ - $^1\text{H}_\alpha$)*	RDC ($^{13}\text{C}_\alpha$ - $^{13}\text{C}'$)*
P2		10.57	
A3		-1.52	
R4		-10.26	-12.00
V5	-0.85	13.24	
G6	2.1	26.71	
L7	0.57	3.05	
G8	0.87		
I9	-5.4		
T10	-0.87	0.45	
V12	-2.49	26.32	
L13	1.04		
T14	-0.7		
T16	2.86		
T17	1.23		
Q18	-0.51	-11.62	
S19	-0.17	7.15	-25.07
S20	0.41	0.72	
G21	0.06		
S22	-0.09	3.83	8.03
R23	0.25		
A24	-0.04		
S25	0.79		
L26	-0.53		
V29	-3.61		
S30	-1.08		
V32	0.23		
L39	-2.35		
V41	0.04		
C42		2.02	-24.26
L43	-1.87		
A49	-0.68		
L50	-0.56		
L51		-2.49	
A54	1.18		
V56	-0.75		
R61	-1.13		
K62	0.35		
R67	0.04		
L68	-0.36		
H71	0.03		
H72	-0.19		

Supporting Information

H73	0.17		
H74	0.11		
H75	0.13		
H76	-0.20		

* The $^{13}\text{C}_\alpha\text{-}^1\text{H}_\alpha$ and $^{13}\text{C}_\alpha\text{-}^{13}\text{C}'$ RDC values are normalized against those of $^{15}\text{N-}^1\text{H}$.

D. TM23 Chemical Shift Differences in Bicelles and in TFE

The chemical shift differences of TM23 residues in $q = 0.5$ bicelles and in TFE are listed in Table S3. As can be seen, chemical shift differences for corresponding residues in TM2 and TM3 are similar when the medium was changed from TFE to bicelle. This suggested that TM2 and TM3 domains of TM23 segments have similar chemical environment changes, indicating that both TM2 and TM3 are embedded in the bicelles.

Table S3. Chemical shift differences of TM23 in bicelles and in TFE

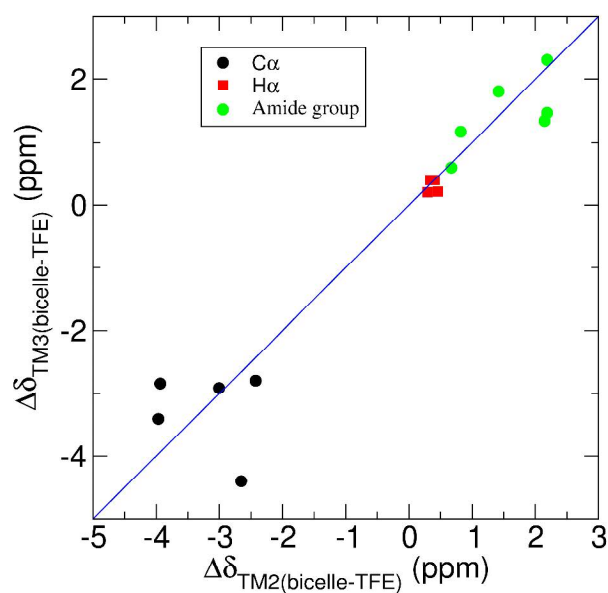
Residue	$\Delta\delta(\text{C}_\alpha)$	$\Delta\delta(\text{H}_\alpha)$	$\Delta\delta(\text{H})$	$\Delta\delta(\text{N})$	$\Delta\delta(\text{amide})^*$
P2	-0.480				
A3	-1.707	0.202	0.891	1.320	1.069
R4	-1.961	0.276	0.830	4.650	2.239
V5	-2.557	0.304	0.776	1.800	1.118
G6	-1.083	0.187	0.596	4.720	2.193
L7	-1.995	0.264	-0.112	-1.850	0.835
G8	-1.236	0.190	0.420	-1.230	0.692
I9	-2.553	0.644	-0.278	-1.560	0.751
T10	-3.004	0.471	0.275	3.110	1.418
T11	-3.936	0.405	-0.114	-4.420	1.980
V12	-2.654	0.409	-0.319	-1.690	0.820
L13	-2.425	0.368	-0.803	-1.540	1.058
T14	-3.966	0.460	-0.254	-4.770	2.148
L15	-2.179	0.292	-0.633	0.510	0.673
T16	-4.964	0.606	-0.534	-3.180	1.519
T17	-5.012	0.500	-0.195	-4.870	2.187
Q18	-2.857	0.361	-0.409	1.310	0.714
S19	-3.014	0.338	-0.031	1.810	0.810
S20	-3.330	0.323	0.372	-1.230	0.664
G21	-1.093	0.658	0.007	1.730	0.774
S22	-3.178	0.300	0.140	-1.680	0.764
R23	-2.643	0.306	0.664	0.840	0.763
A24	-1.131	0.192	0.198	4.870	2.187

Supporting Information

S25	-1.727	0.093	0.487	3.730	1.738
L26	0.183	0.333	0.467	0.680	0.557
V29	-	0.446	0.034	1.430	0.640
S30	-	-0.064	0.370	-1.760	0.870
V32	-	-	-0.044	1.106	0.497
L39	-	-	-0.532	3.060	1.468
C42	-	0.399			
F43	-	-	1.004	4.643	2.306
L50	-	0.206			
L51	-3.405	0.215	0.237	-1.230	0.599
E52	-2.793	-	0.024	3.000	1.342
Y53	-4.402	-			
A54	-2.840	0.401	0.030	2.620	1.172
A55	-2.912	0.051	0.051	6.512	
V56	-	-	-0.154	4.020	1.804

$$* \Delta\delta(\text{amide}) = \sqrt{\Delta\delta(^1\text{HN})^2 + \Delta\delta(^{15}\text{N})^2} / 5$$

Figure S1 below depicts the chemical shift differences in bicelle vs. in TFE for several residues in TM3 as a function of the corresponding chemical shift differences for residues at similar locations in the TM2 domain. Black, $\Delta\delta(\text{C}_\alpha)$; Red, $\Delta\delta(\text{H}_\alpha)$; and Green, $\Delta\delta(\text{amide})$.



E. References

Supporting Information

- (1) Onsager, L. *Annals of the New York Academy of Sciences* **1949**, *51*, 627-659.
- (2) Struppe, J.; Vold, R. R. *J Magn Reson* **1998**, *135*, 541-6.
- (3) Vold, R. R.; Prosser, R. S. *J. Magn. Reson.* **1996**, *B113*, 267-271.
- (4) Glover, K. J.; Whiles, J. A.; Wu, G.; Yu, N.; Deems, R.; Struppe, J. O.; Stark, R. E.; Komives, E. A.; Vold, R. R. *Biophys J* **2001**, *81*, 2163-71.